Experimental Evidence of the 90° Stop Band in the GSI UNILAC

L. Groening, W. Barth, W. Bayer, G. Clemente, L. Dahl, P. Forck, P. Gerhard, I. Hofmann, M. S. Kaiser, M. Maier, S. Mickat, and T. Milosic

GSI Helmholtzzentrum für Schwerionenforschung GmbH, Planckstrasse 1, D-64291 Darmstadt, Germany

D. Jeon

Oak Ridge National Laboratory, Oak Ridge, Tennessee 37830, USA

D. Uriot

CEA IRFU, Service des Accélérateurs, de Cryogénie et de Magnétisme, F-91191 Gif-sur-Yvette, France

(Received 16 March 2009; revised manuscript received 5 June 2009; published 12 June 2009)

In a particle accelerator with a periodic structure beam space charge force may excite resonant beam emittance growth if the particle's transverse phase advance approaches 90°. A recent simulation study with the PARMILA code [D. Jeon *et al.*, Phys. Rev. ST Accel. Beams **12**, 054204 (2009)] has shown the feasibility of measuring the stop band of this fourth order resonance in the GSI Universal Linear Accelerator UNILAC and proposed its experimental verification, which is reported here. Measurements of transverse phase space distributions behind a periodically focusing structure reveal a fourfold symmetry characteristic of fourth order resonances as well as a resonance stop band above $\sigma_0 = 90°$ per focusing cell. These experimental findings agree with results from three different beam dynamics simulation codes, i.e., DYNAMION, PARMILA, and TRACEWIN.

DOI: 10.1103/PhysRevLett.102.234801 PACS numbers: 29.27.Bd, 41.75.−i, 41.85.−p

The possibility of degrading beam quality in high intensity accelerators as a result of the periodically modulated space charge force was recognized a number of years ago. The first systematic and self-consistent theoretical study of such phenomena in linear transport systems showed the existence of stop bands in all orders of perturbations of an initially well-matched Kapchinsky-Vladimirsky (KV) beam [1]. At low intensity (small space charge tune shift) these stop bands are located near resonance conditions of the kind $n\sigma_0 = 180°$ or 360°, with n describing the order. The most prominent case of stop bands resulting from this study has been the so-called envelope instability (near $2\sigma_0 = 180°$) found for a zero current phase advance σ_0 just above 90°. Its existence was studied experimentally in a linear transport experiment in the context of heavy ion inertial fusion [2], which was more recently compared with detailed computer simulation analysis [3].

Avoiding such a $\sigma_0 \geq 90°$ stop band has become a commonly accepted rule of linac design since [4]. Simulation studies of periodic focusing lattices have suggested, however, that the interpretation of this stop band as envelope instability is incomplete for realistic (non-KV) beam distributions, in which case a 4th-order space charge resonance (with $4\sigma_0 = 360°$) dominates over the envelope instability as was shown in Refs. [5,6] in the context of circular accelerator periodic focusing lattices. It should be noted that the same 4th-order space charge resonance may occur in a circular accelerator if the phase advance in the fundamental lattice cell approaches the required condition $4\sigma_0 = 360°$. Its appearance was actually demonstrated experimentally in the KEK proton synchrotron by an observed emittance growth for injection at a tune of $Q = 7.05$ corresponding to $\sigma_0 = 90.64°$ (28 cells per turn), which was explained as 4th-order space charge resonance [7]. A recent theoretical study has shown that this 4th-order space charge resonance also sets important design constraints in a nonscaling fixed field alternating gradient (FFAG) accelerator, where crossing of it may occur due to a large tune swing during acceleration [8].

The present work is the first experimental account of this phenomenon in a linear accelerator. An important condition enabling the current study has been the successful termination of a benchmarking experiment at the UNILAC supported by the European Commission [9] in the years 2006–2008, which led to a visible improvement in mismatch control and confidence in diagnostics [10]. In the course of this benchmarking simulations it turned out that at the UNILAC a measurement of the 4th-order resonance might be feasible [11].

The experiments were done using the first Alvarez type DTL tank of the GSI Universal Linear Accelerator (UNILAC) originally designed for acceleration of $^{238}U^{28+}$ [12] depicted in Fig. 1. The tank comprises 63 rf-gaps accelerating the beam at a synchronous phase of −30° with 108 MHz rf frequency from 1.4 to 3.6 MeV/u. Adjacent rf gaps are separated by a drift tube housing a single quadrupole. The transverse focusing lattice is of the *F-F-D-D* type; i.e., two consecutive quadrupoles are focusing in the same plane followed by two quadrupoles focusing in the other transverse plane. Accordingly, the beam passes 15 full lattice periods within a length of 12 m. In order to provide for sufficiently high phase advances

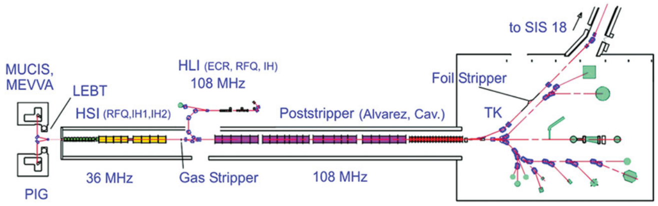

FIG. 1 (color). The Universal Linear Accelerator (UNILAC).

within the quadrupole field limits, the ion $^{40}Ar^{10+}$ was used.

At the UNILAC intense and stable dc beams of $^{40}Ar^{1+}$ are provided by a multicusp ion source with the energy of 2.2 keV/u. Beam bunching and acceleration to 120 keV/u is performed in a radio frequency quadrupole structure followed by two interdigital H-mode cavities providing acceleration to 1.4 MeV/u at 36 MHz. Prior to injection into the DTL the beam passes a nitrogen gas jet for stripping to the charge state of 10+ . Afterwards the beam is matched longitudinally and transversely to the DTL. Figure 2 depicts the matching section comprising a 36 MHz rebuncher, a quadrupole doublet, and a quadrupole triplet with an 108 MHz rebuncher for final adaptation of the beam envelope to the periodic lattice of the DTL. Besides beam matching the section includes diagnostics to determine the beam properties in front of the DTL. Measurements of rms bunch length are performed by detecting secondary electrons emitted by a thin foil intersecting the beam [13]. The electron arrival time on a multichannel plate is related to an rf-master oscillator thus achieving a resolution of 1° at 108 MHz. Horizontal and vertical phase space distributions are measured using a slit-grid device with a resolution of 0.5 mm and 0.5 mrad. Finally, the beam intensity is measured with a beam current transformer. Behind the DTL a quadrupole doublet focuses the beam into a section comprising a slit-grid device for emittance measurements (resolution 1.0 mm/0.7 mrad), a current transformer, and a Faraday cup.

The linac section prior to the DTL was set to deliver a current of 7.1 mA of $^{40}Ar^{10+}$. Using the diagnostics of the matching section the beam properties in front of the DTL were determined. The transverse zero current phase advance σ_0 along the DTL was set through its quadrupole gradients. In order to provide for a $6d$-matched injection into the periodically focusing DTL lattice, the setting of the

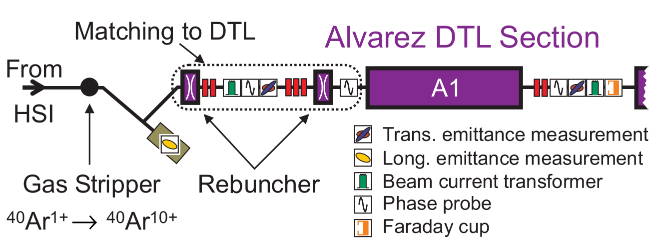

FIG. 2 (color). Schematic setup of the experiments (not to scale).

matching section was adapted to each σ_0 individually. The matching procedure is described in detail in [10]. σ_0 was varied from 60° to 130°, and for each value of σ_0 horizontal and vertical phase space distributions were measured at the DTL exit. Additionally, the beam transformers at the DTL entrance and exit were used to verify full beam transmission.

The method of reconstruction of the beam distribution at the entrance to the 36 MHz rebuncher is defined and experimentally verified in [10]. Its application to the present experiment yields the initial distribution as plotted in Fig. 3. It must be mentioned that the available diagnostics and hence the reconstruction method is not sensitive to eventual correlations among different planes. Being aware of this uncertainty such correlations were assumed to be zero anyway. However, they might drive emittance exchange between correlated planes.

Because of defocusing space charge forces the phase advance experienced by the beam σ is depressed with respect to the zero current phase advance σ_0. The amount of depression depends on the beam current as well as on the emittances in the three planes. Table I presents the depressed tunes for each value of σ_0.

In order to estimate the residual mismatch at the entrance to the DTL the computer code DYNAMION [14] was used. The initial distribution was tracked from the 36 MHz rebuncher to the DTL exit. At the entrance to the DTL the beam Twiss parameters were extracted and compared to

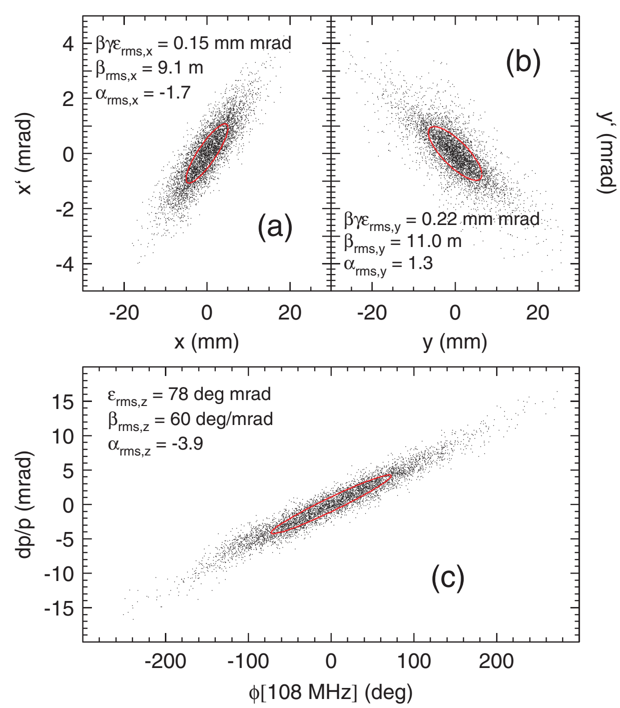

FIG. 3 (color). Horizontal (a), vertical (b), and longitudinal (c) projection of the phase space distribution at the entrance to the 36 MHz rebuncher as used for the simulations. The rms Twiss parameters and the corresponding ellipses are indicated.

TABLE I. Phase advances along the DTL in case of zero current (left) and phase advances for 7.1 mA of $^{40}Ar^{10+}$ (right) for an rms equivalent beam with a KV distribution. The corresponding normalized rms emittances are 0.15/0.22 mm mrad (horizontal/vertical) and 78 deg mrad longitudinally (referring to 108 MHz and to relative momentum deviation). The longitudinal zero current phase advance is constant and 43°.

σ_0 (deg) Transverse	Horizontal	σ (deg) Vertical	Longitudinal
60.0	43.0	45.9	38.3
70.0	52.4	55.5	37.9
79.9	61.8	65.0	37.5
84.8	66.6	69.9	37.4
89.9	71.4	74.7	37.4
95.0	76.3	79.7	37.4
96.0	77.2	80.7	37.4
97.6	78.7	82.2	37.3
100.0	81.1	84.6	37.3
105.0	85.9	89.4	37.2
109.8	90.4	94.0	37.2
119.7	99.9	103.7	37.0
130.0	109.4	113.5	37.0

the periodic solution. The relative mismatch [15] of envelopes is drawn in Fig. 4 as a function of the phase advance σ_0. It is very small transversely, but the relatively large longitudinal mismatch is due to the large initial bunch length exceeding the quasilinear ranges of the two rebunchers in the matching section.

Besides DYNAMION the simulation codes PARMILA [16] and TRACEWIN [17] were used to simulate the complete experiment. After measuring and simulating the transverse phase space distributions at the DTL exit as plotted in Fig. 5, the corresponding rms emittances were evaluated. The mean value of the horizontal and vertical rms emittance, i.e., $\epsilon_{\mathrm{rms},\perp} = (\epsilon_{\mathrm{rms},x} + \epsilon_{\mathrm{rms},y})/2$, is presented in Fig. 6 as a function of the phase advance σ_0.

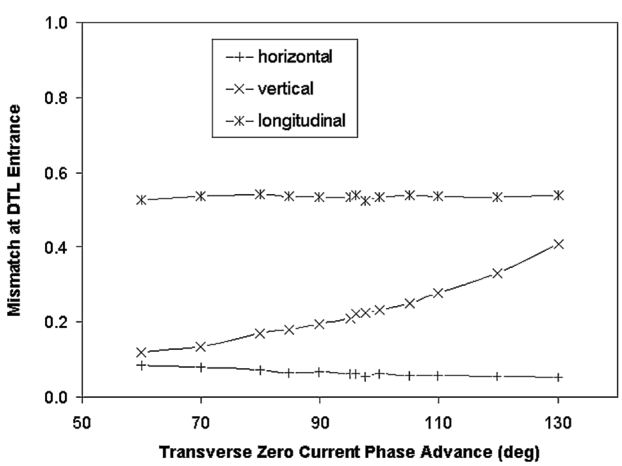

FIG. 4. Residual mismatch of the beam at the DTL entrance as obtained from simulations using the DYNAMION code.

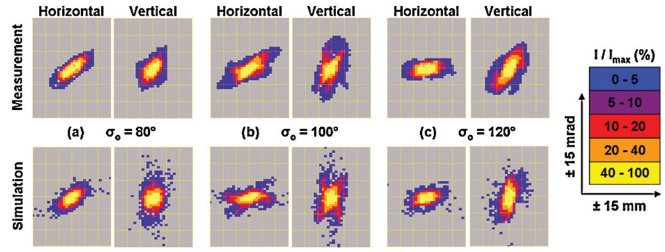

FIG. 5 (color). Upper (lower): phase space distributions at the exit of the DTL as obtained from measurements (simulations using the DYNAMION code) for a transverse zero current phase advance of 80° (a), 100° (b), and 120° (c). Left (right) side plots refer to the horizontal (vertical) plane. The scale is ±15 mm and ±15 mrad. Fractional intensities refer to the phase space element including the highest intensity.

The emittance $\epsilon_{\mathrm{rms},\perp}$ at the DTL exit was found to be independent of the phase advance for values of $\sigma_0 \leq 90°$. Growth was observed for $\sigma_0 \geq 90°$ in both transverse planes. These observations are in very good agreement to the simulations done with three different codes. The measured growth rate of $\epsilon_{\mathrm{rms},\perp}$ is constant for $\sigma_0 \geq 110°$. In the horizontal plane the measured growth disappeared for $\sigma_0 \geq 110°$ while the vertical growth increased, leading to a constant growth for the mean transverse emittance $\epsilon_{\mathrm{rms},\perp}$. The codes reproduced the behavior in the horizontal plane but they delivered reduced growth beyond the resonance also in the vertical plane. This disagreement might be due to unknown residual correlations between the two transverse planes in the initial distribution being not included into the simulations as mentioned above.

Distributions corresponding to phase advances far away from the stop band have elliptical shapes (Fig. 5). At $\sigma_0 \approx 100°$ instead the measurements and the simulations clearly revealed four arms, which are typical for a resonant 4th-order interaction—here due to space charge.

This confirms the existence of a resonance stop band as predicted in previous theoretical work [6,11]. The experi-

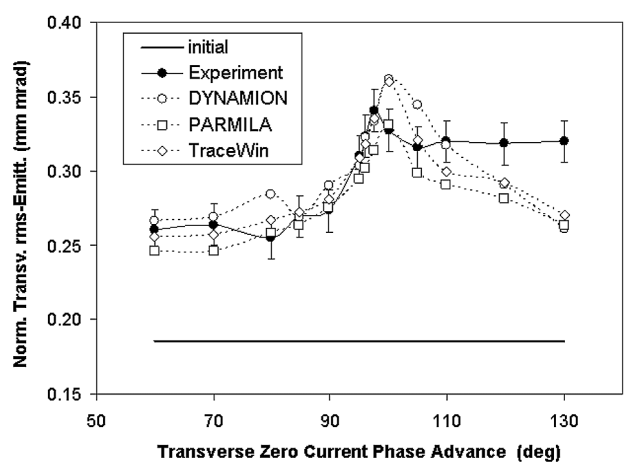

FIG. 6. Mean of horizontal and vertical rms emittance as a function of the transverse zero current phase advance along the DTL.

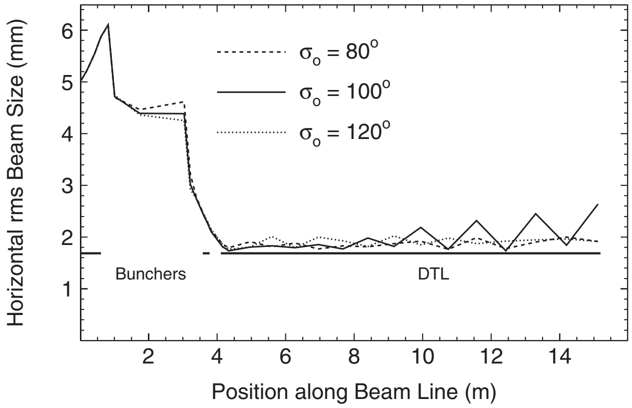

FIG. 7. Horizontal rms beam envelope along the beam line for three different phase advances as simulated using DYNAMION.

mental stop band is well confirmed by simulation results using the actual linac structure. The exact width of the stop band depends on the type of periodic focusing—it is zero for constant focusing. A necessary condition is $\sigma_0 \geq 90°$; according to the theoretical analysis of Ref. [1] the width shrinks linearly to zero with the space charge tune shift $\sigma_0 - \sigma$. In our case the stop band width is approximately given by $\sigma_0 - \sigma \approx 20°$. For phase advances above the resonance the measurements revealed a constant $\epsilon_{\mathrm{rms},\perp}$ higher than below, while the simulations predicted a decreasing slope. To verify whether the asymmetric behavior of $\epsilon_{\mathrm{rms},\perp}$ around the resonance is due to the increased residual mismatch at higher σ_0, simulations with a perfectly matched beam starting at the entrance of the DTL were performed. The results revealed the same asymmetric behavior as observed in the simulation of the experiment with slightly mismatched beams. To estimate the impact of the envelope instability, transverse rms beam sizes delivered by the DYNAMION code have been evaluated along the beam line. Figure 7 plots the horizontal beam width for three different phase advances. Also for $\sigma_0 = 120°$ no envelope instability is observed. The envelope ripple at 100° is driven by the 4th-order resonance.

During the preparation of the experiments simulations using a KV distribution with similar rms emittances and equal rms mismatch to the DTL have been done. They revealed very low rms emittance growth of less then 10%. Since KV distributions do not have a 4th-order space charge potential, this demonstrates that for the measured emittance growth the 4th-order resonance dominates over the envelope instability as predicted in [11]. Probably the envelope instability needs significantly more periods to develop with respect to the resonance. Hence these measurements are the first direct evidence of a 4th-order space charge driven resonance in a linear accelerator. They thus offer a rigorous experimental basis for the 90° stop band, which has so far been used in design consideration on theoretical grounds only.

We acknowledge the support of the European Community-Research Infrastructure Activity under the FP6 ''Structuring the European Research Area'' programme (CARE, Contract No. RII3-CT-2003-506395). The participation of D. Jeon to this work was made possible partly by the support of ORNL/SNS (managed by UT-Battelle, LLC, for the U.S. Department of Energy under Contract No. DE-AC05-00OR22725).

[1] I. Hofmann, L. J. Laslett, L. Smith, and I. Haber, Part. Accel. **13**, 145 (1983).
[2] M. G. Tiefenback and D. Keefe, IEEE Trans. Nucl. Sci. **32**, 2483 (1985).
[3] S. M. Lund and B. Bukh, Phys. Rev. ST Accel. Beams **7**, 024801 (2004).
[4] M. Reiser, *Theory and Design of Charged Particle Beams* (John Wiley & Sons Inc., New York, 1994), p. 240.
[5] I. Hofmann, in *Proceedings of the Workshop on the Use of the Spallation Neutron Source for Heavy Ion Fusion Beam Dynamics Studies, Abingdon, 1981* (unpublished), p. 77.
[6] I. Hofmann, G. Franchetti, and A. Fedotov, in *Proceedings of the 20th ICFA Advanced Beam Dynamics Workshop on High Intensity and High Brightness Hadron Beams, Batavia, Illinois*, AIP Conf. Proc. No. 642 (AIP, New York, 2002), p. 248.
[7] S. Igarashi, T. Miura, E. Nakamnura, Y. Shimosaki, M. Shirakata, K. Takayama, and T. Toyama, in *Proceedings of the 29th ICFA Advanced Beam Dynamics Workshop on Beam Halo Dynamics, Diagnostics, and Collimation HALO'03, Montauk, New York*, AIP Conf. Proc. No. 693 (AIP, New York, 2003), p. 114.
[8] S. Y. Lee, G. Franchetti, I. Hofmann, F. Wang, and L. Yang, New J. Phys. **8**, 291 (2006).
[9] http://care.lal.in2p3.fr/.
[10] L. Groening, W. Barth, W. Bayer, G. Clemente, L. Dahl, P. Forck, P. Gerhard, I. Hofmann, G. Riehl, S. Yaramyshev, D. Jeon, and D. Uriot, Phys. Rev. ST Accel. Beams **11**, 094201 (2008).
[11] D. Jeon, L. Groening, and G. Franchetti, Phys. Rev. ST Accel. Beams **12**, 054204 (2009).
[12] W. Barth, L. Dahl, L. Groening, J. Glatz, S. Richter, and S. Yaramyshev, in *Proceedings of the XXII Linac Conference, Lübeck, 2004*, edited by V. R. W. Schaa (DESY, Hamburg, Germany, 2004), p. 246.
[13] P. Forck, F. Heymach, T. Hoffmann, A. Peters, and P. Strehl, in *Proceedings of the XX Linac Conference, Monterey, 2000* (SLAC, Menlo Park, 2000), p. 166.
[14] S. Yaramyshev, W. Barth, L. Groening, A. Kolomiets, and T. Tretyakova, Nucl. Instrum. Methods Phys. Res., Sect. A **558**, 90 (2006).
[15] T. P. Wangler, *Rf Linear Accelerators* (John Wiley & Sons Inc., New York, 1998), p. 217.
[16] J. H. Billen and H. Takeda, Los Alamos National Laboratory, Report No. LAUR-98-4478, 1998 (unpublished) (revised 2004).
[17] http://irfu.cea.fr/Sacm/logiciels/index.php